Available online at www.sciencedirect.com
SCIENCE DIRECT®

Journal of the European Ceramic Society 23 (2003) 603–611

www.elsevier.com/locate/jeurceramsoc

# Influence of additives content on the high temperature oxidation of silicon nitride based composites

R. Klein[a,*], V. Medri[b], M. Desmaison-Brut[a], A. Bellosi[b], J. Desmaison[a]

[a]*SPCTS, CNRS, UMR 6638, University of Limoges, 123 Av. A. Thomas 87060 Limoges, France*
[b]*CNR-IRTEC, National Research Council, Research Institute for Ceramic Technology, Via Granarolo 64, 48018 Faenza, Italy*

Received 4 October 2001; accepted 7 October 2002

**Abstract**

A life prediction tool for mechanical and electrical applications of electroconductive structural ceramics is essential in order to know the limit for engineering uses. The aim of this work was to study the influence of additives content on the oxidation behaviour, in pure oxygen between 900 and 1400 °C, of two fully dense $Si_3N_4$–35 vol.% TiN composites. For this purpose, a hot pressed material (HP), containing 3.7 wt.% of $Y_2O_3$ and $Al_2O_3$ as sintering aids, was compared to an hipped material (HIP), containing 0.4 wt.% of the same additives. Up to a temperature $T < \sim 1200$ °C, where the oxidation of the composite is mainly governed by the preferential oxidation of TiN, the two materials exhibit paralinear kinetics with very close oxidation resistance. Contrarily, the hipped material shows a better oxidation resistance at $T > \sim 1200$ °C, when the oxidation of the $Si_3N_4$ matrix takes place. The formation of a compact silica sub-scale acts as an efficient diffusion barrier leading to asymptotic kinetics, with final weight gains exhibiting a negative temperature dependence. In the case of the HP material, i.e. in presence of a higher content of additives, a deterioration of the protective nature of the scale is provoked by the increased mobility of the impurity cations ($Y^{3+}$, $Al^{3+}$) linked to a decrease of the viscosity of the secondary glassy phase. The kinetics have a paralinear shape up to 1400 °C, with final weight gains increasing as a function of temperature. Therefore, this study confirms the deleterious influence on oxidation resistance of additives used for a better sintering of powders and the beneficial effect of hot isostatic pressing for which lower amounts of aids are necessary in comparison with hot pressing.
© 2003 Elsevier Science Ltd. All rights reserved.

*Keywords:* Composites; Corrosion; HIP; HP; $Si_3N_4$; TiN

## 1. Introduction

Thanks to their strength, hardness and thermal stability, silicon nitride based ceramics are among the most interesting materials for structural applications. In the last years, significant attention has been devoted to particulate-reinforced ceramics. The addition of an electrically conductive secondary phase such as TiN, TaN, TiCN, $TiB_2$, TiC, $MoSi_2$..., to the brittle $Si_3N_4$ ceramics has been recognized as a positive relevance for specific applications in the field of high temperature heaters, igniters and heat exchangers.[1–15] The manufacture of complex shape components is possible because the high electrically conductivity facilitates electrical discharge machining (EDM).[1,4,16,17]

In view of the potential applications where the materials are exposed to high temperature under oxidizing environment, the thermal stability of the composites is one of the most important properties to be evaluated.

It is well known from the literature that the oxidation of silicon nitride-based materials and composites strongly depends on the microstructure: porosity, impurities, grain boundary phases.[18–23] In many cases, parabolic kinetics indicating diffusion processes as rate-controlling mechanisms stress the decisive role of the grain boundary phases. Nevertheless, in some cases, non-parabolic kinetics were observed. Many open arguments, despite plentiful published data, still wait to be completely clarified. In the case of electroconductive composites, the oxidation is also affected by the presence (type and amount) of easy-to-oxidize main

* Corresponding author. Tel.: +33-5-55-45-75-40; fax: +33-5-55-45-76-48.
*E-mail address:* robert.klein@unilim.fr (R. Klein).

0955-2219/03/$ - see front matter © 2003 Elsevier Science Ltd. All rights reserved.
PII: S0955-2219(02)00376-X

secondary phases.[1–5,24–34] The oxidation of $Si_3N_4$–TiN composites results in different behaviours and oxidation mechanisms depending on the temperature,[26–28,31] the silicon nitride matrix microstructure and the amount of TiN particles. Chemical reactions leading to the oxidation of TiN[25] and of $Si_3N_4$[24] are accompanied by several diffusive phenomena. Therefore the complex interactions among the involved species at the reaction interface and inside the growing oxide scale and the development of complex product layers affect the overall oxidation behaviour.

In this study, the oxidation behaviour of two dense $Si_3N_4$ + 35 vol.% TiN composites was considered. The same silicon nitride (Baysinid, average diameter: 0.15 μm) and titanium nitride (H.C. Starck, grade C, average diameter: 1.2 μm) were used. One fully dense HP material, containing 3.68 wt.% of $Y_2O_3 + Al_2O_3$ as sintering aid, was compared to a HIP composite, containing 0.4 wt.% of the same additives. Oxidation kinetics were recorded in the temperature range 900–1400 °C under dry flowing oxygen. On the basis of weight gains and morphological examinations of the oxidized surfaces and cross sections, a clarification based on the factors influencing the oxidation, the reactions and diffusive phenomena and on the rate controlling steps is proposed putting an emphasis on the role of processing conditions (HP or HIP) and additives content.

## 2. Experimental procedure

### 2.1. Materials

The sintering procedure and parameters are indicated in Table 1.

The same following TiN, $Si_3N_4$, $Y_2O_3$ and $Al_2O_3$ powders were used to elaborate the composite materials. The experimental processing procedures were the following ones:

- for the HIP composite, the four powders were dispersed by ultrasonic assistance in ethanol, then the mixture was dried at 100 °C, sieved at 32 μm and cold isostatically pressed (dr # relative density: # 60%). The crude cylinder was introduced inside a silica container and sealed.
- for the HP composite, the TiN powder was dispersed by ultrasonic assistance with ethanol, then the suspension was mixed with $Al_2O_3$, $Y_2O_3$ and silicon nitride in a plastic jar with $Si_3N_4$ milling media and ethanol for 24 h. The powder mixture was dried in a rotating evaporator under $N_2$ atmosphere.

The density was measured by using Archimedes principle. The microstructures of the two fully dense composites are compared in Fig. 1a,b. A good dispersion of the two phases is noticed. No reaction has occurred between the two powders during the sintering and the phase transformation α- to β-$Si_3N_4$ was over 95% in both cases.

### 2.2. Oxidation tests

Oxidation tests were carried out on cubic samples (4×4×4 $mm^3$) which were polished up to 1 μm and cleaned with ethanol. The weight gain was recorded with a SETARAM microbalance.

The non-isothermal oxidation tests from room temperature up to 1400 °C (heating rate 2 °C/min) were done in flowing oxygen (5 l/h).

In the case of isothermal experiments (temperature range 900–1400 °C, for 24 h), the heating up stage was performed with a constant argon flux of 5 l/h and the sample was introduced inside the isothermal zone at the selected temperature in order to avoid preliminary oxidation.

Microstructural analysis of surfaces and cross-sections of oxidized samples were carried out by X-ray diffraction (XRD), scanning electron microscope (SEM) and EDS microanalysis.

## 3. Results

The two composite materials start to oxidize above 700 °C (Fig. 2) and the weight gain is only detectable above 800 °C. The weight increase observed at 1200 °C

Table 1
Elaboration parameters ($Si_3N_4$ + 35 vol.% TiN)

| | Sintering aids | | | | | | | Sintering cycle | $d_{relative}$ (%) |
|---|---|---|---|---|---|---|---|---|---|
| | Baikowski | Merck | $Si_3N_4$ Baysinid impurities | | | TiN Stark C Impurities | | | |
| | $Al_2O_3$, | $Y_2O_3$, | O | Fe | Al | O | Fe | | |
| **HIP** | **0.13 wt.%** | **0.26** | 1.44 wt.% | 5.3 ppm | 10 ppm | 1.5 wt.% | 0.1 wt% | Hot isostatic pressing (HIP) 1725 °C, 1 h, vacuum, 180 MPa | 100 |
| **HP** | **1.05 wt.%** | **2.63** | | | | | | Hot pressing (HP) 1800 °C, 10 min, vacuum, 30 MPa | 100 |

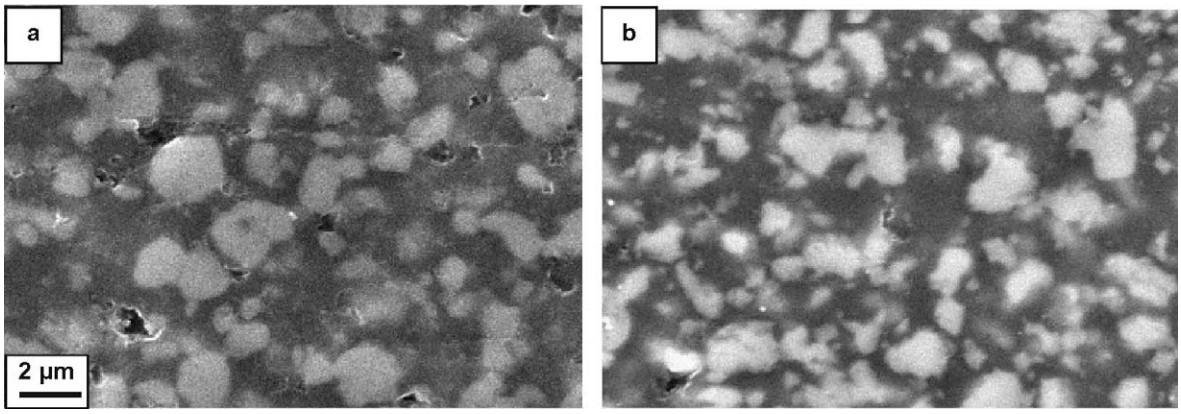


Fig. 1. SEM images of the HP (a) and HIP (b) polished surfaces.

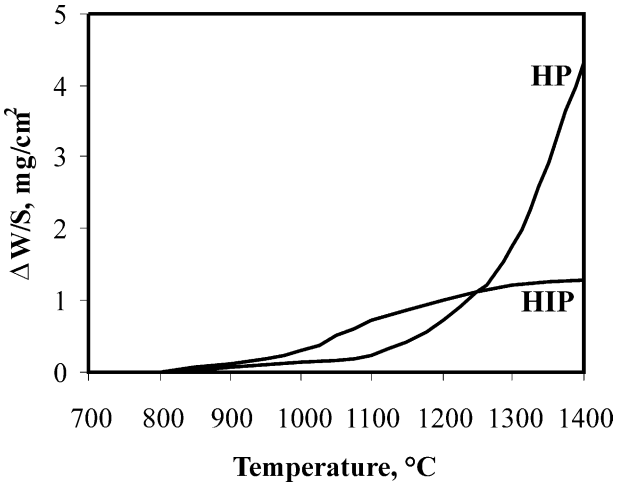


Fig. 2. Non-isothermal oxidation curves obtained in flowing oxygen (heating rate 2 °C/min).

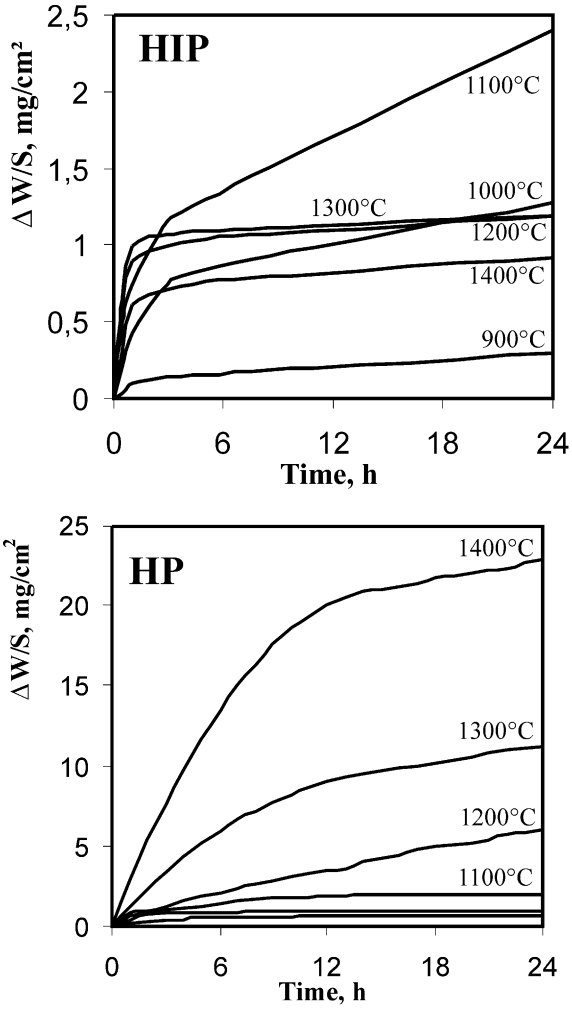


Fig. 3. Isothermal kinetic curves obtained between 900 and 1400 °C in flowing oxygen.

and above is more important for the HP composite than for the HIP composite.

Concerning the isothermal tests, the mass variations per surface area resulting from the oxidation tests in the temperature range 900–1400 °C have been plotted against time (Fig. 3). The HIP composite is slightly less resistant up to 1100 °C, while at $T \geqslant 1200$ °C, its resistance is much higher.

For the HIP composite, the oxidation kinetics exhibit a paralinear shape up to 1100 °C and become asymptotic above this temperature with plateaux characterized by weight gains decreasing as a function of temperature. Conversely, for the HP composite, the kinetics are always paralinear and the final weight gains are increasing in all the temperature range. In order to proceed to a rough comparison of the reactivity of these two materials, it was assumed that their kinetics were both following an initial transitory parabolic stage, during a 5 h period below 1200 °C in the case of the HIP composite and between 2 and 13 h within the temperature range 900–1400 °C for the HP material, respectively. The values of $k$ reported as a function of temperature on the Arrhenius curve (Fig. 4) were obtained by plotting the weight gain per unit area ($\Delta W/S$) against time ($t$) according to the parabolic law:

$$(\Delta W/S)^2 = kt + b$$

where $k$ ($mg^2\ cm^{-4}\ h^{-1}$) is the parabolic rate constant, $S$ is the area of the surfaces exposed to oxidation, b stands for the occurrence of a first non parabolic stage. The decrease of $S$ with time, in the case of cubic samples, has been neglected and a pseudo-planar symmetry has been assumed due to the low extent of the material conversion. The results (Fig. 4) show that the oxidation behaviour of these two materials is very similar in the temperature range 900–1100 °C and corresponds to an apparent activation energy values ($E_a$) of 236 kJ/mol. They also reveal a substantial increase in the value of $E_a$ (362 kJ/mol) for the HP material, between 1200 and 1400 °C.

The evolution of oxidized surfaces with temperature is compared in Fig. 5a–f. In the case of the HIP sample, in the whole temperature range 900–1400 °C, crystalline $TiO_2$ is detected by XRD on the surface. However the rounded shape of the rutile grains, observed after oxidation at 1400 °C (Fig. 5e), indicates the formation of a liquid phase embedding the crystals. A small silica peak (cristobalite) is also detected at the highest temperatures (1300–1400 °C).

On the oxidized surface of HP samples, up to 1100 °C only rutile is detected as a crystalline phase, while at $T \geqslant 1200$ °C, α-cristobalite is also present. A glassy phase re-covers massively the oxide after 24 h treatment at 1400 °C.

The cross section analysis of the oxidized samples reveals, for both materials, titanium depletion in the sublayer beneath the reaction interface between the oxide scale and the bulk material. At 1000 °C (Fig. 6a,b), a low amount of oxygen is only detected in this sublayer, related to a slight oxidation of $Si_3N_4$ and the probable formation of a silicon oxynitride phase (Fig. 6a).

At 1200 °C (Fig 6c,d), a higher oxygen content is detected in this sublayer, indicating the enhancement of the reaction between silicon nitride and oxygen.

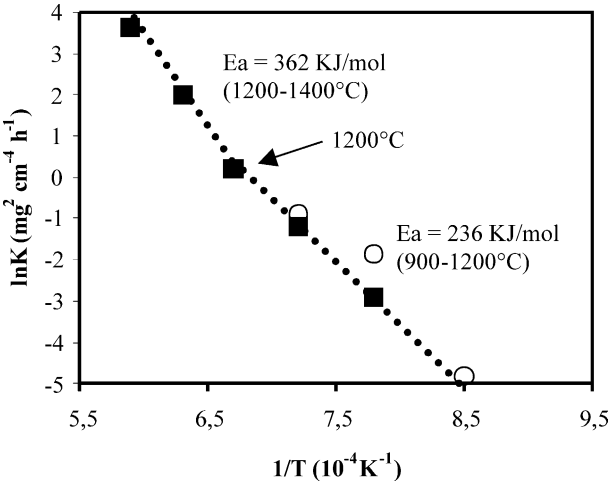


Fig. 4. Influence of temperature on the rate constant $k$ at 1 atm, HIP(○) and HP(■).

In all the samples, the limit between the bulk and the sublayer is not clearly identified, as a complex multilayered microstructure with a compositional gradient is established from the unreacted bulk material to the external oxidized surface. These features are enhanced with the increase of the oxidation temperature. It is particularly evident on the cross section micrograph of the HP sample treated at 1400 °C (Fig. 7a), where the multilayered structure can be approximately schematized on the basis of the following different oxide zones from the surface in contact with the atmosphere towards the bulk:

1. A porous oxide scale, where cristalline $TiO_2$ and cristobalite crystals are embedded into a siliceous glassy phase, containing yttrium near the surface (Fig. 7b) and certainly aluminum and impurity cations present in the starting powders.
2. Beneath it, a more compact layer mainly constituted with $TiO_2$ and $SiO_2$ where large $TiO_2$ inclusions are formed by aggregation of individual $TiO_2$ grains located at the interface with the porous oxide scale. At the internal limit, yttrium is found with titanium as a line of white spots which may be presumably yttrium titanate (Fig. 7a,b).
3. A Ti-depleted sublayer rich in $SiO_2$ and certainly $SiN_xO_y$, is depleted from the additive cations, particularly yttrium. Pores are concentrated in the middle of this zone, leading to the formation of cracks. But a difference in thermal expansion coefficient and the rapid cooling of the sample after the oxidation test may have led to this failure.

Concerning the HIP cross section, two main zones may be observed (Fig. 8): a dense rutile external layer and an internal porous titanium depleted zone. No presence of yttrium is noticed, the amount of yttria introduced is too low.

In both cases, the bulk material shows a progressively decreasing concentration of Ti in the areas approaching the reaction interface, due to the outward titanium migration.

## 4. Discussion

Up to 1100 °C the oxidation resistance of the HP composite is slightly higher than the resistance of the HIP material. At 1100 °C, the weight gain value is about the same, while at 1200 °C the final weight gain value ($\Delta W/S$) of the HP material is five times greater than the HIP value. Consequently, as it has already been claimed in the literature, the compositional effect, mainly the sintering aids amount, has a great influence on the oxidation.

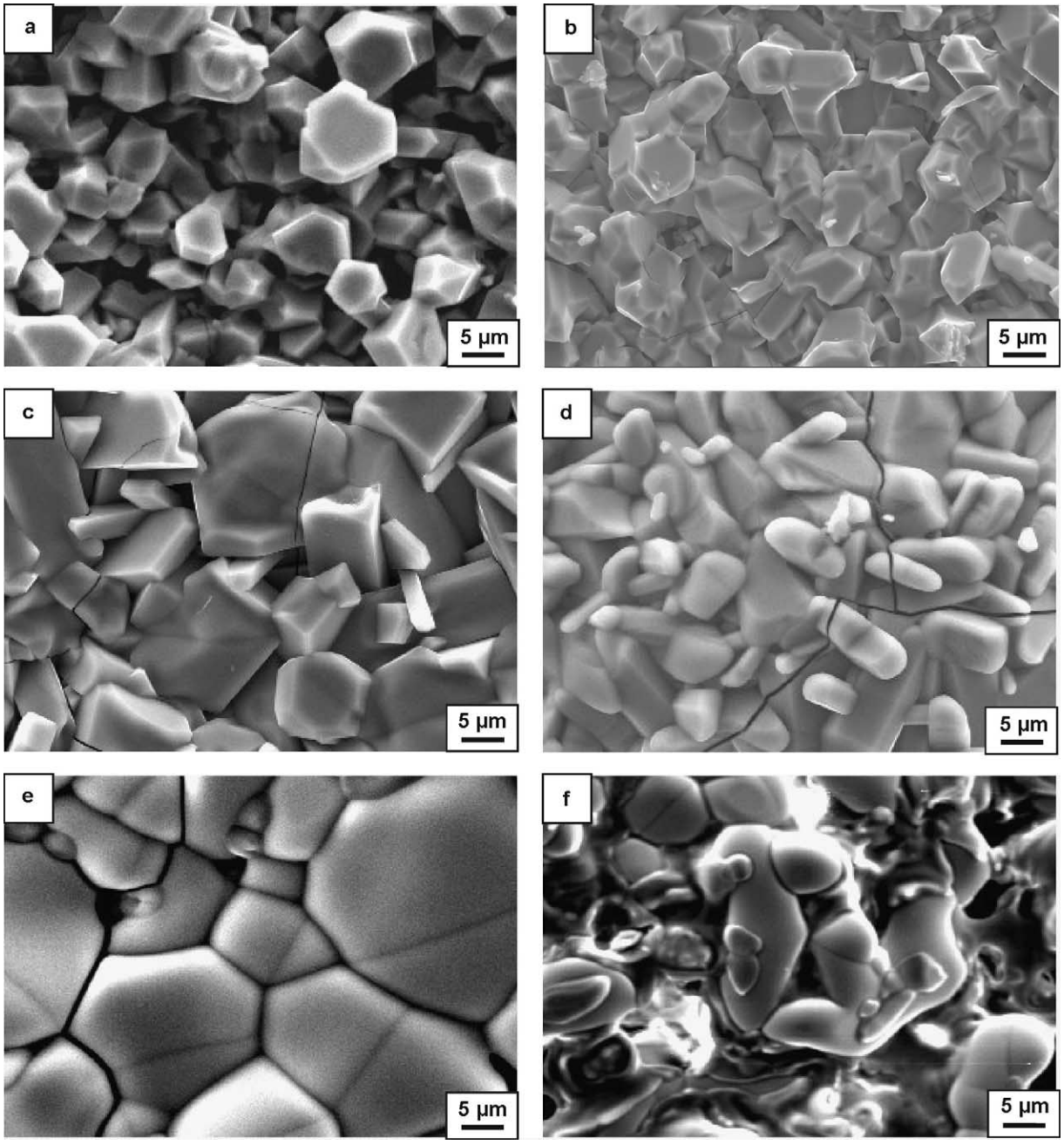


Fig. 5. SEM images of the oxide surfaces after 24 h of oxidation at 1000 °C (a, b), 1200 °C (c, d), 1400 °C (e, f) of HIP (left) and HP (right) composites respectively.

From 900 to 1100 °C, the oxidation behaviour of the $Si_3N_4$–35 vol.% TiN composites is mainly concerned with the preferential oxidation of TiN, according to the reaction (1)

$$TiN_s + O_{2g} \rightarrow TiO_{2s} + 1/2N_{2g} \quad (1)$$

The oxidation of silicon nitride is very slow and difficult to detect by XRD below 1100 °C.

It is well known[26–28] that the formation of the Ti depleted sublayer is due to Ti migration, which takes place during the early stages of the oxidation process. TiN particles are rapidly oxidized and the kinetic mechanism is mainly governed by the diffusion of Ti through $TiO_2$: this oxidation period finishes when titanium migration is stopped by porosity in the sublayer.

Globally, the mechanism which has already been proposed[28,35] between 1000–1200 °C is confirmed. In a first step, the oxidation of the TiN phase is controlled by the outward diffusion of Ti through $TiO_2$ rutile which creates pores. After the formation of a porous sublayer, the oxidation of inner TiN grains is controlled by the inward diffusion of oxygen through $TiO_2$.

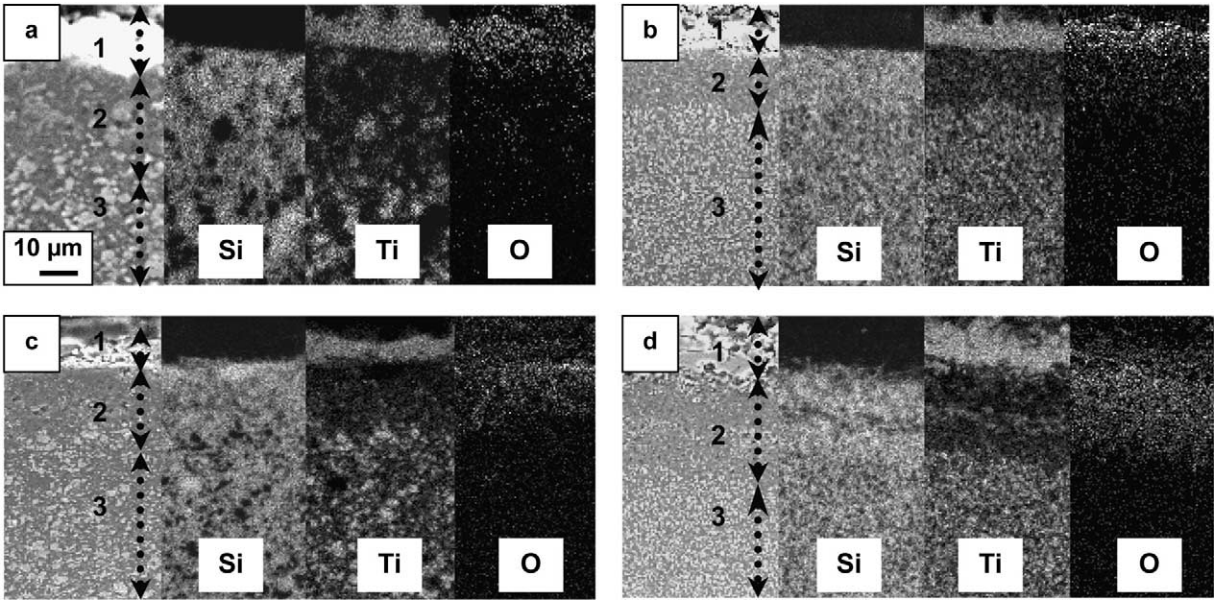


Fig. 6. SEM images and EDS maps of Si, Ti, O after 24 h of oxidation at 1000 °C (a, b) and 1200 °C (c, d) of the HIP and HP multilayered cross sections respectively: (1) external oxide scale; (2) titanium depleted sublayer; (3) bulk material.

At $T > 1200$ °C, a higher amount of oxygen is noticed in the sublayer beneath the rutile scale and cristobalite ($SiO_2$) is also detected in the oxide scale of both materials. Besides reaction (1), the oxidation of $Si_3N_4$ becomes consistent, leading to the formation of a higher quantity of $SiO_2$, according to reaction (2)

$$Si_3N_4 + 3O_2 \rightarrow 3SiO_2 + 2N_2 \quad (2)$$

During subsequent oxidation, the difference of yttrium concentration between the surface oxide and the bulk causes the outward diffusion of $Y^{3+}$ and certainly $Al^{3+}$ ions (but Al is not so easy to detect). As a result of this outward diffusion of cations to the surface, Y-depletion occurs in the sublayer, as previously observed,[21–23,33] and the oxide scale is enriched with glassy or crystalline yttrium-titanates/silicates and silica. The silicon nitride grains oxidize progressively and silica fills in the porosity of the internal sublayer which becomes a diffusion barrier for later oxidation.

On the basis of the above reported results, the high temperature behaviour of $Si_3N_4$–35vol.%TiN is affected by:[25–28]

- the presence of TiN, which is an easy-to-oxidize phase at temperatures higher than about 600 °C,[25,27]
- the intergranular phase, as in a similar study on the oxidation of the dense monolithic HIP $Si_3N_4$ with the same amount of aids,[24] the sintering aids has been proved to largely diffuse as cations toward the reaction interface, to interact with $Si_3N_4$ oxidation products, mainly $SiO_2$, forming a glassy silicate phase ($Y_2SiO_7$) rather important on the surface above 1450 °C. In our case, it seems that yttrium titanate ($Y_2Ti_2O_7$) is prevalent (Fig. 7b). Composition and amount of these silicate phases play a crucial role, acting as high diffusivity paths for the gaseous species ($O_2$ and $N_2$). Consequently, a driving force exists as a step towards adjusting the composition of the silicates[21,23] surface layer. These phenomena are related to the amount of grain boundary phase in the starting material and exert considerable influence at temperatures which lower the viscosity of the liquid phase, therefore favouring a better wettability of the $Si_3N_4$ and a demixing process.

This is particularly evident for the HP samples oxidized at 1400 °C, containing a relatively high content of sintering aids. The enhanced oxidation resulted in the formation of glassy phases, which are located all along the grain boundaries embedding the $TiO_2$ grains. On the contrary, the oxidation of the HIP samples was slower due to the very low amount of sintering aids which resulted only in the presence of a limited amount of a viscous $SiO_2$ liquid phase at the grain boundaries.

Therefore, the limitation of the additive quantity in the HIP material enables an important decrease of the oxidation rate, above 1200 °C, by formation of more compact silica sub-scale acting as an efficient diffusion barrier leading to asymptotic kinetics. The change in apparent activation energy ($E_a$) observed on the Arrhenius plot around this temperature is linked to the higher content of additives present in the HP material which increases the mobility of active species within the oxide scale by decreasing the secondary glassy phase viscosity. In addition, the formation of pores propagating in the

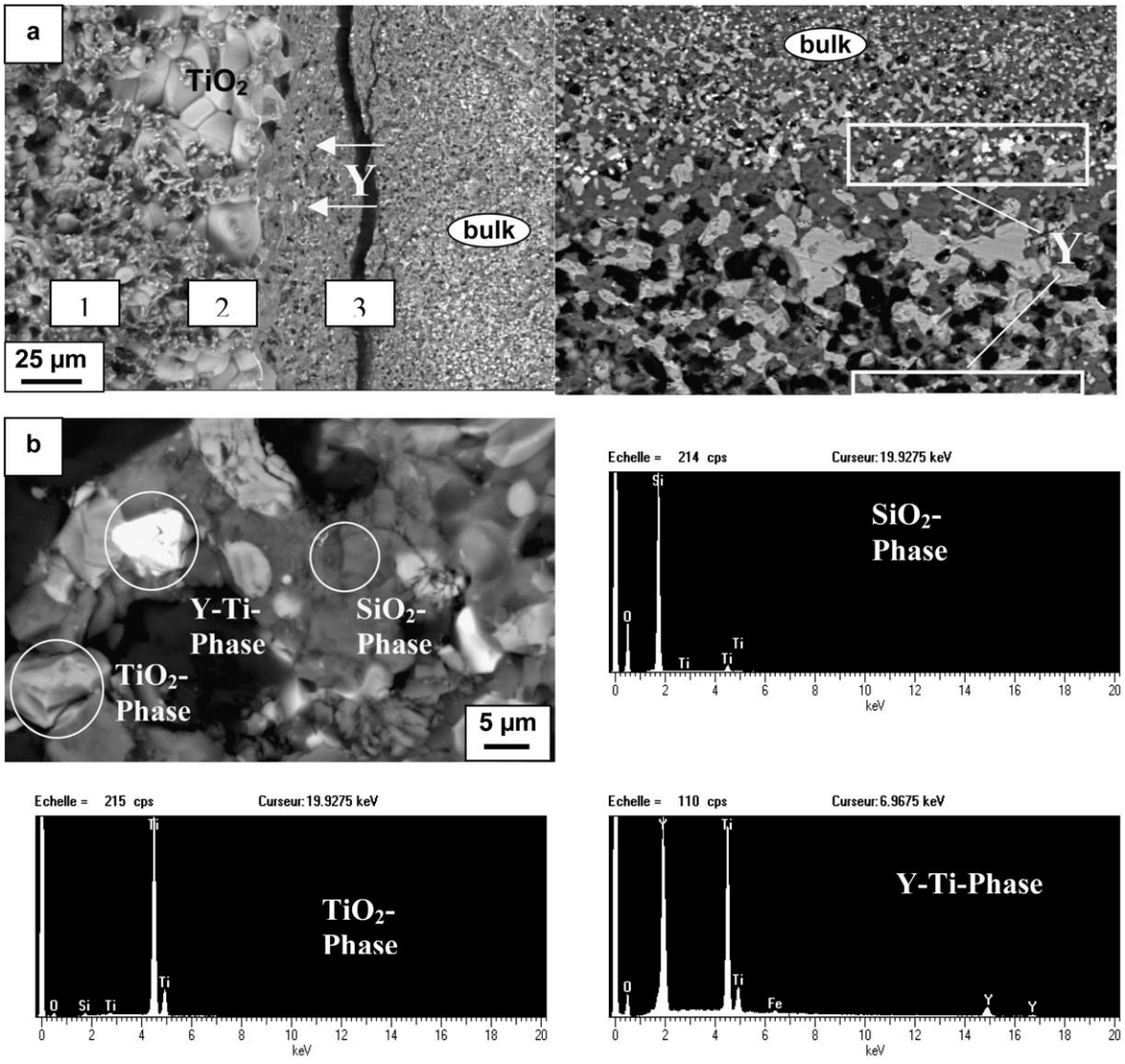


Fig. 7. (a) SE and BSE images of the multilayered cross section of the HP sample after 24 h of oxidation at 1400 °C with two lines of a Y–Ti phase and (b) BSE image and EDS analysis of grains in the outer part of the oxide layer similar to the inner part.

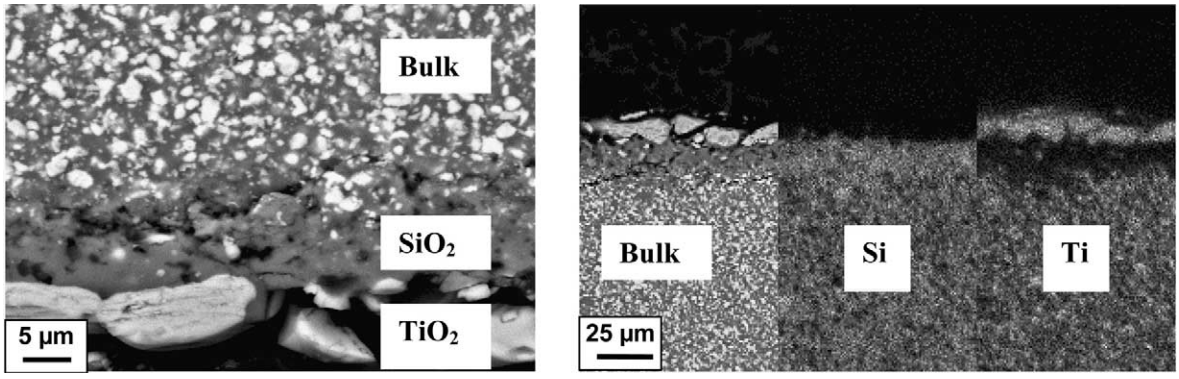


Fig. 8. BSE image and EDS analysis of the multilayered cross section of the HIP sample after 24 h of oxidation at 1400 °C.

sublayer allows fast transport of $O_2$ and $N_2$. The paralinear shape of the kinetics reflects the evolution of the contribution of these phenomena with time.

## 5. Conclusion

The oxidation behaviour, in dry oxygen, of two $Si_3N_4$–35 vol.% TiN composites, either hot pressed (HP) or hot isostatic pressed (HIP), with different amounts of sintering aids, was compared in the temperature range 900–1400 °C. Concerning the HP composite, whose oxidation kinetics are paralinear, the oxide scales are complex due to the formation of a multilayered structure. An external oxide zone $TiO_2$ rich contains silica/silicate phases whose quantity increases with temperature. An internal sublayer is titanium depleted and rather porous. Two lines of Y–Ti grains are noticed on cross sections which confirm the outward migration of cations.

Up to 1200 °C, where the oxidation of TiN is prevailing, the oxidation resistance of the two materials is very closed. On the other hand, above 1200 °C, where the oxidation of the silicon nitride matrix becomes relevant, a degradation of the resistance the HP composite is provoked by the increased mobility of the impurity cations ($Y^{3+}$, $Al^{3+}$) linked to a decrease of the viscosity of the secondary glassy phase. Conversely, the HIP material shows an improved resistance due to a more protective silica rich sub-layer. Thus diffusion of active species (inward O, outward N, Ti) is limited.

Consequently, for the low-doped (HIP) composite, the oxidation kinetics which are paralinear up to 1100 °C, with final weight gains increasing with temperature., become asymptotic, between 1200 and 1400 °C, with final weight gains exhibiting a negative temperature dependence.

Therefore, this study confirms the deleterious influence of additives used for a better sintering of powders and the beneficial effect of hot isostatic pressing for which less aids are necessary than in the case of hot pressing.

## Acknowledgements

The authors would like to thank Dr. D. Tétard and P. Carles (both from the University of Limoges) for their technical assistance. We greatly acknowledge the support of the European Community in the frame of the European Network Project –Corrosion of ceramic matrix composites–HPRN-CT-2000-00044.

## References

1. Gogotsi, Yu.G., Review-particulate silicon nitride-based composites. *J. Mat. Sci*., 1994, **29**, 2541–2556.
2. Huang, J.-L., Chen, S.-Y. and Lee, M.-T., Microstructure, chemical aspects and mechanical properties of $TiB_2/Si_3N_4$ and TiN/$Si_3N_4$ composites. *J. Mater. Res*., 1994, **9**(9), 2349–2353.
3. Huang, J.-L., Lee, M.-T., Lu, H-H. and Lii, D-F., Microstructure, fracture behaviour and mechanical properties of TiN/$Si_3N_4$ composites. *Mat. Chem. and Phys*., 1996, **45**, 203–210.
4. Bellosi, A., Guicciardi, S. and Tampieri, A., Development and characterization of electroconductive $Si_3N_4$-TiN composites. *J. Eur. Ceram. Soc*., 1992, **9**, 82–93.
5. Nagaoka, T., Yasuoka, M., Hirao, K. and Kanzaki, S., Effects of TiN particle size on mechanical properties of $Si_3N_4$–TiN particulate composites. *J. Ceram. Soc. Jpn*., 1992, **100**, 617–620.
6. Zivkovic, L. M., Boskovic, S. M. and Miljkovic, S., Sintering behaviour and microstructure development in electroconductive $Si_3N_4$-TiN composites. In *Advanced Science and Technology of Sintering*, ed. Stojenovich *et al*. Kluwer Academic/Plenum Publishers, New York, 1999, pp. 475–481.
7. Akimune, Y., Munakata, F., Hirosaki, N. and Okamoto, Y., Optimization of mechanical and electrical properties of TiN/$Si_3N_4$ material by agglomerates-microstructure control. *J. Ceram. Soc. Jpn*, 1998, **106**, 77–80.
8. Petyrovsky, V. Y. and Rak, Z. S., Densification, microstructure and properties of electroconductive $Si_3N_4$–TaN composites. Part I: densification and microstructure. *J. Eur. Ceram. Soc*., 2001, **21**, 219–235.
9. Petyrovsky, V. Y. and Rak, Z. S., Densification, microstructure and properties of electroconductive $Si_3N_4$-TaN composites. Part II: electrical and mechanical properties. *J. Eur. Ceram. Soc*., 2001, **21**, 237–244.
10. Herrmann, H., Balzer, B., Schubert, C. and Hermel, W., Densification, microstructure and properties of $Si_3N_4$–TiCN composites. *J. Eur. Ceram. Soc*., 1993, **12**, 287–296.
11. Huang, J.-L. and Chen, S.-Y., Investigation of silicon nitride composites toughened with prenitrided $TiB_2$. *Ceram. Int*., 1995, **21**, 77–83.
12. Shew, B.-Y. and Huang, J.-L., Investigation of chemical reactions in $TiB_2/Si_3N_4$ composites. *Mat. Sci. Eng*., 1992, **A159**, 127–133.
13. Petrovich, J. J., Pena, M. I. and Kung, H., Fabrication and microstructures of $MoSi_2$-$Si_3N_4$ matrix composites. *J. Am. Ceram. Soc*., 1997, **80**, 111–116.
14. Petrovich, J. J., Pena, M. I., Reimanis, I. E., Sandlin, M. S., Conzone, S. D., Kung, H. H. and Butt, D. P., Mechanical behaviour of $MoSi_2$ reinforced-$Si_3N_4$ matrix composites. *J. Am. Ceram Soc*., 1997, **80**, 3070–3076.
15. Kao, M., Properties of silicon nitride-molybdenum disilicide particulate ceramic composites. *J. Am. Ceram Soc*., 1993, **76**, 2879–2883.
16. Martin, C., Cales, B., Vivier, P. and Mathieu, P., Electrical discharge machinable ceramic composites. *Mat. Sci Eng*., 1989, **A109**, 351–356.
17. Liu, C.-C. and Huang, J.-L., Micro-electrode discharge machining of TiN/$Si_3N_4$ composites. *Brit. Ceram. Trans*., 2000, **99**, 149–152.
18. Ogbuji, L. U. T., The $SiO_2$-$Si_3N_4$ interface, part 1: nature of the interphase. *J. Am. Ceram Soc*., 1995, **78**, 1272–1278.
19. Ogbuji, L. U. T., The $SiO_2$-$Si_3N_4$ interface, part II: $O_2$ permeation and oxidation reaction. *J. Am. Ceram. Soc*., 1995, **78**, 1279–1284.
20. Chen, J., Sjöberg, J., Linquist, O., O'Meara, C. and Pejryd, L., The rate controlling processes in the oxidation of hipped silicon nitride with and without sintering additives. *J. Eur. Ceram. Soc*., 1991, **7**, 319–327.
21. Backhaus-Ricoult, M. and Gogotsi, Yu., Identification of oxidation mechanisms in silicon nitride ceramics by transmission electron microscopy studies of oxide scales. *J. Mat. Res*., 1995, **10**(9), 2306–2321.
22. Nickel, K. G., Multiple law modelling for the oxidation of

advanced ceramics and a model-independent figure of merit. In *Corrosion of Advanced Ceramics: Measurement and Modelling, NATO-ASI Series, Vol 267*, ed. K. G. Nickel. Kluwer Academic, Dordrecht, 1994, pp. 73–84.
23. Monteverde, F. and Bellosi, A., High oxidation resistance of hot pressed silicon nitride containing yttria and lanthania. *J. Eur. Ceram. Soc.*, 1998, **18**, 2313–2321.
24. Themelin, L., Desmaison-Brut, M. and Billy, M., Oxidation behaviour of a hot isostatically pressed silicon nitride material. *J. Phys. IV*, 1993, **3**, 881–888.
25. Desmaison-Brut, M., Bianchi, L., Schneider, S. V., Themelin, L. and Desmaison, J., Oxidation behaviour of an AlN-TiN composite material and comparison with the dense monolithic ceramics. In *Materials Science Forum, High Temperature Corrosion and Protection of Materials IV, Vol. 2*, ed. R. Streiff, J. Stringer, R. C. Krutenat, M. Caillet and R. A. Rapp. Trans Tech Publications, Swizerland, 1997, pp. 899–906.
26. Bellosi, A., Tampieri, A. and Y-Zhen, L., Oxidation behaviour of electroconductive $Si_3N_4$-TiN composites. *Mat. Sci. Eng.*, 1990, **A127**, 115–122.
27. Graziani, T., Baxter, D. J. and Bellosi, A., The oxidation of $Si_3N_4$–TiN ceramics in air–1vol% $SO_2$. In *Key Engineering Materials* Vol. 113. Trans Tech Publication, Switzerland, 1996, pp, 123–134.
28. Deschaux-Beaume, F., Cutard, T., Fréty, N. and Levaillant, C., Oxidation of a silicon nitride–titanium nitride composite: microstructural investigations and phenomenological modeling. *J. Am. Ceram. Soc.*, 2002, **85**(7), 1860–1866.
29. Tampieri, A., Bellosi, A. and Biasini, V., Oxidation resistance of $Si_3N_4$–$TiB_2$ composites. In *Advanced Structural Inorganic Composites*. ed. P. Vincenzini. Elsevier Science 1991, pp. 409–420.
30. Klemm, H., Tangermann, K., Schubert, C. and Hermen, W., Influence of molybdenum silicide additions on high temperature oxidation resistance of silicon nitride materials. *J. Am Ceram. Soc.*, 1996, **79**, 2429–2475.
31. Desmaison, J. and Desmaison-Brut, M., High temperature kinetics of non-oxide monolithic and particulate composite ceramics. *Mater. Sci. Forum*, 2001, **369-372**, 39–54.
32. Gogotsi, Yu., Oxidation resistance of $Si_3N_4$–TiN ceramics. In *Proc. Eur. Ceram. Soc. 2nd Conf.*, Vol. 2, ed. G. Ziegler and M. Hausner, Augsbourg 1991, pp. 1517–1521.
33. Themelin, L., Desmaison-Brut, M. and Billy, M., Post-densification behaviour of pressureless sintered silicon nitride materials: relationship between properties and microstructure. *Ceramics International*, 1992, **18**, 119–130.
34. Desmaison-Brut, M. and Billy, M., High temperature corrosion of hot pressed silicon nitride materials. In *High Temperature Corrosion of Technical Ceramics*, ed. R. Fordham, Elsevier Applied Science, 1990, pp. 131-140.
35. Deschaux-Beaume, F., Fréty, N., Cutard, T. and Colin, C., A phenomenological model for high temperature oxidation of $Si_3N_4$-TiN composites. *Materials Science Forum*, 2001, **368-372**, 403–410.